The "hype" in hyperpolarized MR: Metabolic imaging using ^{13}C MR

Jan Wolber, René in 't Zandt, Mathilde Lerche, Mikkel Thaning, Andreas Gram, Rolf Servin, Björn Fridlund, Fredrik Ellner, Jan Henrik Ardenkjaer-Larsen, Klaes Golman,

GE Healthcare Bio-Sciences, Medical Diagnostics R&D,
Medeon, 205 12 Malmö, Sweden

Introduction

The fate of organic molecules has been studied extensively by NMR both *in vitro* and *in vivo*. With this approach important information about metabolism and preference of substrates at different pathological conditions can be revealed (see for example (1-5)). Despite significant technological advancements (increasing field strength and improved coil design), the application of such studies is, however, limited by an intrinsically low sensitivity and long experiment times. Thus, these approaches do not enable functional imaging in the sense of being able to track real-time changes in metabolism of a substance present in near-physiological concentration.

Fundamentally, the low sensitivity originates from the low magnetic energy of nuclear spins, compared to the thermal energy at room temperature, which leads to a low spin polarization even in the strongest NMR magnets. For instance, at a magnetic field strength of 1.5 T and room temperature, ^{13}C spins are polarized to only 1.3 ppm, and an improvement of several orders of magnitude is thus theoretically possible. A range of methods have been proposed to enhance the polarization of nuclear spins (denoted hyperpolarization methods), e.g. brute force by applying high magnetic field strengths and going to temperatures close to zero Kelvin (see also Appendix, equation A5)), optical pumping of noble gases (see for example (6), para-hydrogen induced polarization (PHIP) (7-9), and Dynamic Nuclear Polarization or DNP in short (10,11). All these methods have demonstrated the potential of creating non-thermal polarization close to unity.

In this contribution, we endeavor to give a brief overview on the application of DNP to generate highly polarized ^{13}C-enriched substrates for *in vivo* MR. We will show that this technology allows true molecular imaging. Most excitingly, metabolism can be tracked by MR, thus enabling a novel approach for assessing tissue viability based on cellular function.

^{13}C hyperpolarization by DNP and technical considerations

DNP is carried out in the solid state in order to create large nuclear polarizations. At a temperature 1 K and in a field of 3 T, the thermal ^{13}C polarization is still far from unity (polarization < 0.1%), but electrons are highly polarized (>90%) due to the much larger γ of the electron (c.f. Appendix Eq. A2). If molecules carrying unpaired electrons (commonly referred to as radicals) are frozen together with a ^{13}C-

containing substance, it is possible to partially transfer polarization to the nuclear spins by irradiating the sample with microwaves close to the electron resonance frequency (10,11). The Microwave irradiation establishes coupling between the electronic and nuclear spin reservoirs, thus increasing the ^{13}C nuclear polarization in the solid material to typically 20% or more under these conditions. For DNP to be efficient, it is adamant that the radical and the ^{13}C-containing substrate are intimately mixed. This is achieved if crystallization is avoided, i.e. if the DNP sample forms an amorphous solid.

The large non-equilibrium polarization needs to be preserved during rapid dissolution of the solid sample. The solid can be transformed into an injectable liquid, with small to negligible polarization losses (see (10)). Figure 1 below illustrates the enormous enhancement in sensitivity for ^{13}C by this method. For a detailed description of the polarization apparatus see (10).

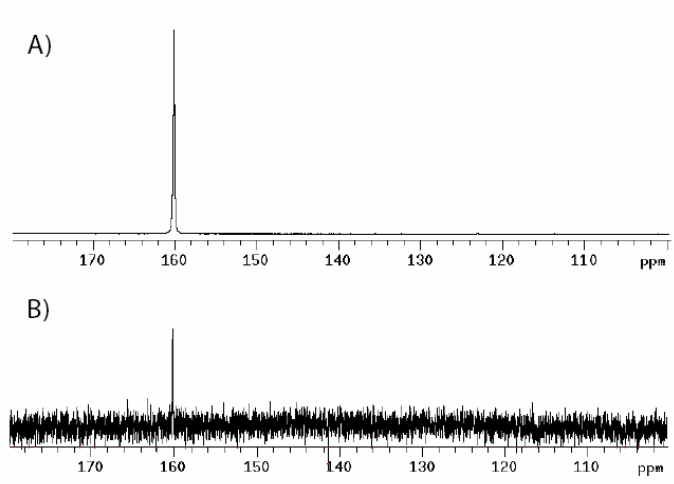

Figure 1: A) ^{13}C spectrum of urea (natural abundance ^{13}C) hyperpolarised by the DNP-NMR method. The concentration of urea was 59.6 mM and the polarisation was 20% (SNR=4592). B) Thermal equilibrium spectrum of the same sample at 9.4 T and room temperature, SNR=7. This spectrum is acquired under Ernst angle conditions (pulse angle of 13.5° and repetition time of 1 s based on a T_1 of 60 s), with full ^{1}H decoupling. The signal is averaged during 65 hours (232,128 transients) (Figure adapted from (10)).

In addition to the chemical requirements for carrying out DNP in the solid state, probes for hyperpolarized ^{13}C MR have to have sufficiently long T_1 relaxation time in the liquid state. Working with ^{13}C-enriched substrates, it is thus necessary to determine which site should be labeled in order to give the most favorable conditions. Obviously, the window of opportunity is given by the timescale of the non-equilibrium polarization decaying back to thermal equilibrium.

Furthermore, a number of biological requisites have to be met as well; the compound may be an endogenous or endogenous substance, but it has to reach the target tissue on the timescale of T_1 and be taken up in cells. Most importantly, a suitable ^{13}C-enriched substrate should exhibit MR sensitivity to its chemical environment. Such changes should be reflected in the ^{13}C chemical shift in order to be detected by hyperpolarized ^{13}C MR. The tool of choice to evaluate different kind of probes using hyperpolarized ^{13}C in the living tissue is spectroscopic imaging or chemical shift imaging (for an excellent description of spectroscopic imaging see (12)).

Another area where a new mindset is required is the MR acquisition strategy. As the large polarization generated by DNP is non-renewable, the MR sequences employed for hyperpolarized MR have to make efficient use of the magnetization. The acquisition time window is limited by T_1; thus, the data need to be acquired rapidly. A small molecule labeled with ^{13}C in the carbonyl position will generally have a sufficiently long T_1 *in vivo*. Apart from T_1 relaxation, T_2, T_2* and diffusion or flow also influence the panel of applications for hyperpolarized imaging techniques. The field dependence of T_2, T_2* is critical for the choice of field strength and imaging strategy.

^{13}C-pyruvate: A probe for ^{13}C metabolic imaging

An example of a molecule meeting the requirements for hyperpolarized ^{13}C MR is pyruvate. Pyruvate is a key molecule involved in glycolysis. It is taken up by cells through a diffusion facilitated transport system (MCT), and its metabolic pathways are well characterized; its main metabolites *in vivo* are alanine, lactate, and bicarbonate. Pyruvate is thus ideally suited to probe LDH activity, and to distinguish aerobic and anaerobic metabolism (see Figure 2).

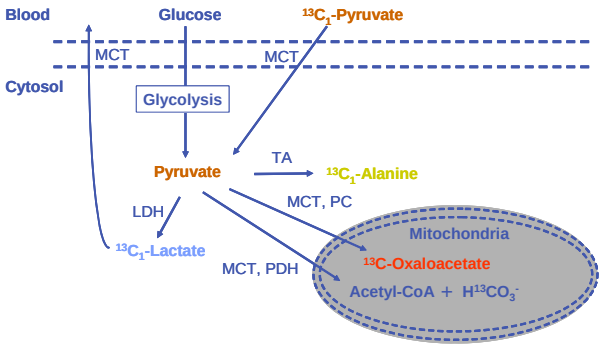

Figure 2: Schematics of intracellular pyruvate metabolism. Abbreviations are: LDH: lactate dehydrogenase, PDH: pyruvate dehydrogenase, PC: pyruvate carboxylase, MCT: monocarboxylic acid transporter, TA: transaminase.

The key requirement for conducting real metabolic imaging is rapid turnover of the substrate whilst the non-equilibrium polarization is available. As can be seen in Figure 3, this is indeed the case, making it possible to study the fate of pyruvate in real time upon injection. In all experiments reported here, 1-^{13}C-pyruvate has been used. The rationale for enriching the carboxyl-carbon is given by its relatively long liquid-state T_1 in aqueous solution of nearly one minute, and by the ability to distinguish pyruvate and its metabolite from the chemical shift of their 1-^{13}C MR resonances. The preservation of the polarization during the enzyme reaction is yet another non-trivial requisite for successful ^{13}C MR metabolic imaging. In complementary *in vitro* experiments using enzyme solutions, we established that the metabolic conversion of the substrate is not associated with any significant loss of polarization.

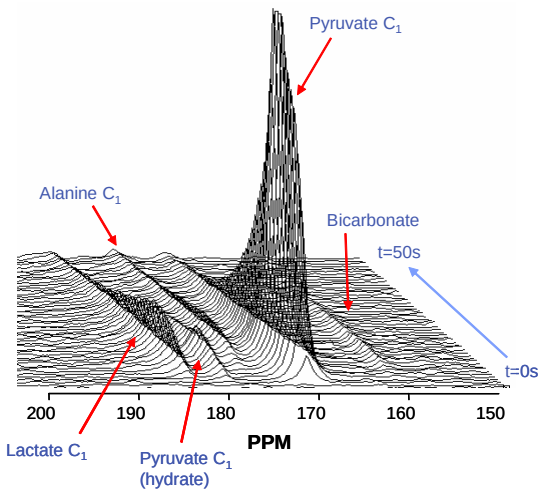

Figure 3: Time series of whole-body ^{13}C MR spectra (every 3 s) after injection of 3 ml of hyperpolarised Na-1-^{13}C-pyruvate solution into the tail vein of a rat. The data were acquired on a clinical 1.5 T MR system.

Interpreting the data in Figure 3, the initial up-slope shows the wash-in of the substrate. The metabolically inactive hydrate form is in equilibrium with pyruvate. Rapidly after injection, lactate and alanine are formed, as well as bicarbonate upon entering the Krebs cycle in the mitochondria. The decay of the pyruvate signal is thus a function of both ^{13}C T_1 relaxation and metabolic turnover. Based on this time series, the best time for spatially resolved acquisitions can be determined. The most obvious strategy is to perform standard spectroscopic imaging with somewhat reduced flip angle. However, spectroscopic imaging is not a fast imaging technique due to only one RF-pulse per repetition time and the high amount of phase encoding steps needed. Thus, the information obtained will reflect the average intensity of the signals during the acquisition window.

We have performed hyperpolarized ^{13}C MR studies with pyruvate in both healthy and diseased animals in order to demonstrate the potential of this exiting new modality. Amongst others, we have studied rats bearing P22 tumors. An example of such a spectroscopic imaging exam is shown in Figure 4, where metabolic maps of pyruvate, alanine, and lactate have been computed from the spectral MR data and superimposed on the ^{1}H MR reference image.

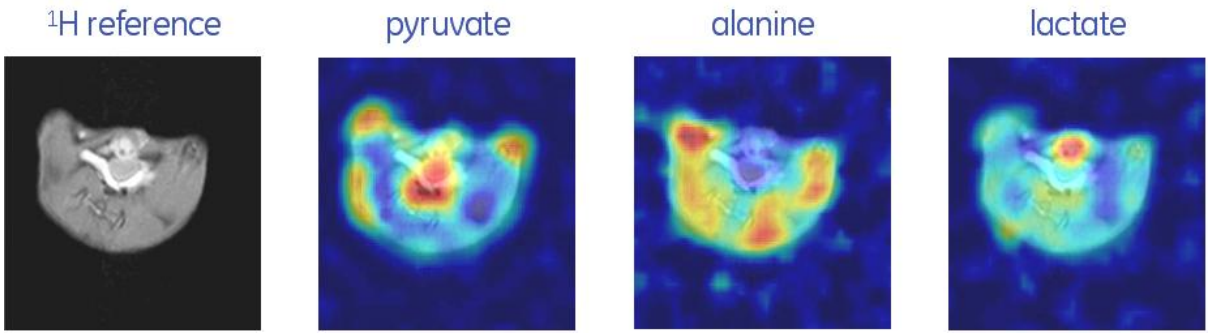

Figure 4: Hyperpolarized ^{13}C MR in a rat bearing a P22 tumor. The metabolic maps were computed from the spectroscopic imaging data by time-domain analysis of the individual spectra.

Improved imaging strategies

Spectroscopic imaging is initial the method of choice to acquire the full ^{13}C MR spectrum. Obviously, the repetition time should be as short as possible. With repetition times of 100 ms or less, sufficient time is available to acquire a MR spectrum with high enough spectral resolution to identify the metabolites. This means that a 16x16 matrix with weighted k-space sampling can be acquired in about 15 seconds. This is fast enough to map the metabolic pattern over a volume of interest. The generation of metabolic maps by quantifying the metabolite MR signals in the spectra requires more advanced fitting routines. The best approach appears to quantify metabolite levels using time domain fitting procedures that overcome the limitations of the frequency domain in this specific application (see for example (14-16).

Higher matrix sizes cannot be reached in a reasonable amount of time. Furthermore, the RF- pulse angle would have to be reduced even more to preserve polarization. Other approaches, such as the Dixon method (13), may be employed, provided all frequencies of interest are known in advance. Further, long T_2 relaxation times may be exploited using multi-echo MR imaging sequences with EPI readouts. A 90-180 echo train would make it possible to image the same volume in a much higher resolution in seconds, provided that the T_2 is long enough and a work-up would be available to reconstruct the metabolite specific MR images (17-20) This new type of sequences specially engineered to image the compound and its metabolites would enable clinical use of ^{13}C-imaging due to its relative simplicity and applicability.

Conclusion

The introduction of injectable, hyperpolarized ^{13}C-substances (10,21,22) opens a new field of MR imaging. MRI in conjunction with hyperpolarized ^{13}C-labelled imaging tracers allows true molecular MR imaging to be performed *in vivo* (21). This novel platform technology will offer radiologists new information of importance for medical diagnosis and treatment. The exciting prospect of probing cellular metabolism with the resolution of MR will provide valuable diagnostic information at a molecular level.

References

1. Ross B, Lin A, Harris K, Bhattacharya P, Schweinsburg B. Clinical experience with 13C MRS in vivo. NMR Biomed 2003;16(6-7):358-369.
2. de Graaf RA, Mason GF, Patel AB, Behar KL, Rothman DL. In vivo 1H-[13C]-NMR spectroscopy of cerebral metabolism. NMR Biomed 2003;16(6-7):339-357.
3. Gruetter R, Adriany G, Choi IY, Henry PG, Lei H, Oz G. Localized in vivo 13C NMR spectroscopy of the brain. NMR Biomed 2003;16(6-7):313-338.
4. Wiechert W. An introduction to 13C metabolic flux analysis. Genet Eng (N Y) 2002;24:215-238.

5. Shulman RG, Rothman DL. 13C NMR of intermediary metabolism: implications for systemic physiology. Annu Rev Physiol 2001;63:15-48.
6. Goodson BM. Nuclear magnetic resonance of laser-polarized noble gases in molecules, materials, and organisms. J Magn Reson 2002;155(2):157-216.
7. Bowers CR, Weitekamp DP. Parahydrogen and synthesis allow dramatically enhanced nuclear alignment. J Am Chem Soc 1987;109:5541-5542.
8. Bowers CR, Weitekamp DP. Transformation of symmetrization order to nuclear spin magnetization by chemical reaction and nuclear magnetic resonance. Phys Rev Lett 1986;57:2645-2648.
9. Golman K, Axelsson O, Johannesson H, Mansson S, Olofsson C, Petersson JS. Parahydrogen-induced polarization in imaging: subsecond (13)C angiography. Magn Reson Med 2001;46(1):1-5.
10. Ardenkjaer-Larsen JH, Fridlund B, Gram A, Hansson G, Hansson L, Lerche MH, Servin R, Thaning M, Golman K. Increase in signal-to-noise ratio of > 10,000 times in liquid-state NMR. Proc Natl Acad Sci U S A 2003;100(18):10158-10163.
11. Abragam A, Goldman M. Principles of dynamic nuclear polarisation. Rep Prog Phys 1978;41:395-467.
12. de Graaf RA. In vivo NMR spectoscopy: principles and techniques; 1998.
13. Dixon WT. Simple proton spectroscopic imaging. Radiology 1984;153(1):189-194.
14. Vanhamme L, van den Boogaart A, Van Huffel S. Improved method for accurate and efficient quantification of MRS data with use of prior knowledge. J Magn Reson 1997;129(1):35-43.
15. Vanhamme L, Sundin T, Hecke PV, Huffel SV. MR spectroscopy quantitation: a review of time-domain methods. NMR Biomed 2001;14(4):233-246.
16. in 't Zandt H, van Der Graaf M, Heerschap A. Common processing of in vivo MR spectra. NMR Biomed 2001;14(4):224-232.
17. Posse S, Tedeschi G, Risinger R, Ogg R, Le Bihan D. High speed 1H spectroscopic imaging in human brain by echo planar spatial-spectral encoding. Magn Reson Med 1995;33(1):34-40.
18. Reeder SB, Faranesh AZ, Atalar E, McVeigh ER. A novel object-independent "balanced" reference scan for echo-planar imaging. J Magn Reson Imaging 1999;9(6):847-852.
19. Reeder SB, Wen Z, Yu H, Pineda AR, Gold GE, Markl M, Pelc NJ. Multicoil Dixon chemical species separation with an iterative least-squares estimation method. Magn Reson Med 2004;51(1):35-45.
20. Wieben O, Leupold J, Speck O, Hennig J. EPSI reconstruction for multi-echo balanced SSFP imaging. 2004; Copenhagen.
21. Golman K, Olsson LE, Axelsson O, Mansson S, Karlsson M, Petersson JS. Molecular imaging using hyperpolarized (13)C. Br J Radiol 2003;76 Suppl 2:S118-127.
22. Golman K, Ardenkjaer-Larsen JH, Petersson JS, Mansson S, Leunbach I. Molecular imaging with endogenous substances. Proc Natl Acad Sci U S A 2003;100(18):10435-10439.